The current issue and full text archive of this journal is available at
www.emeraldinsight.com/0961-5539.htm

Numerical simulation of natural convection in a partitioned enclosure using PDQ method

Kamil Kahveci
Faculty of Engineering and Architecture, Trakya University, Edirne, Turkey

Received 10 September 2005
Revised 12 June 2006
Accepted 30 June 2006

Abstract

Purpose – This paper seeks to investigate the effect of a heat conducting vertical partition in an enclosure on natural convection heat transfer and fluid flow using the polynomial-based differential quadrature (PDQ) method.

Design/methodology/approach – The PDQ method with the non-uniform Chebyshev-Gauss-Lobatto grid point distribution given below is used to transform the governing equations into a set of algebraic equations. After numerical discretization, the resulting algebraic equations are solved by the successive over-relaxation iteration method.

Findings – It is found that the average Nusselt number decreases towards a constant value as the partition is distanced from the hot wall towards the middle of the enclosure. Furthermore, with decreasing thermal conductivity ratio, the average Nusselt number first increases and passes a peak point and then begins to decrease. The average heat transfer rate exhibits little dependence on the width of the partition in the range taken into consideration in this study for the thickness of the partition.

Originality/value – This study offers more knowledge on natural convection in partitioned enclosures.

Keywords Convection, Polynomials, Vortices

Paper type Research paper

Nomenclature

a = first-order weighting coefficient
b = second-order weighting coefficient
g = gravitational acceleration, m^2/s
H = height of the enclosure, m
k = thermal conductivity, W/(mK)
L = width of the enclosure, m
N = the number of partitions
Nu = Nusselt number
Pr = Prandtl number
p = dimensionless pressure
R = residual
Ra = Rayleigh number
r_k = the ratio of thermal conductivities
r_w = dimensionless thickness of the partition
T = dimensionless temperature
u = dimensionless horizontal velocity
v = dimensionless vertical velocity
w = thickness of the partition, m
x = dimensionless horizontal coordinate
y = dimensionless vertical coordinate
α = thermal diffusivity, m^2/s
β = thermal coefficient of volume expansion, 1/K
ΔT = dimensionless temperature difference between the vertical walls of the enclosure
υ = kinematic viscosity, m^2/s
η = outward direction normal to the surface
ρ = density, kg/m^3
ω = dimensionless vorticity
ψ = dimensionless stream function

Subscripts

a = average
b = partition
C = cold
f = fluid
H = hot
o = evaluated at reference temperature

Superscripts

* = dimensional quantities

International Journal of Numerical Methods for Heat & Fluid Flow
Vol. 17 No. 4, 2007
pp. 439-456

0961-5539
DOI 10.1108/09615530710739194

1. Introduction

Thermal convection in enclosures has many engineering applications, such as solar collectors, energy transfer in rooms and buildings, cooling of electronic equipments and energy storage. The problem of primary interest in the previous studies is that of a simple rectangular enclosure[1]. However, real systems can differ significantly from a simple rectangular enclosure model in certain respects. For example, in some building applications, the transfer of heat through a vertical wall that separates adjacent rooms must be coupled with natural convection in both rooms. Some of the electronic equipments have a vertical wall separating two adjacent enclosures. In this case, the model must include the association of these two enclosures communicating laterally through the vertical wall. The case is similar for the solar collector where the convection in the two adjacent air layers is coupled at the glazing. These and the possible insulating effect of partitions are some of the reasons which encouraged researchers to turn their attention to the study of convection in enclosures with partitions.

Available studies of natural convection in a partitioned enclosure are concerned mostly with the vertically partitioned case. Ho and Yih (1987) studied the problem numerically for an air-filled enclosure with a centrally located partition and concluded that the heat transfer rate attenuates considerably in a partitioned enclosure in comparison with that observed in a non-partitioned enclosure. The results of Tong and Gerner (1986) show that placing a partition exactly midway between the vertical walls of an enclosure produces the greatest reduction in heat transfer. A study by Dzodzo *et al.* (1999) on natural convection for an enclosure with a centrally located partition indicates that partitioning the enclosure decreases the convective heat transfer up to 64 percent. Karayiannis *et al.* (1992) found that the finite conductivity of the partition causes an increase in the Nusselt number. Acharya and Tsang (1985) found that inclination angle of an enclosure with a centrally located partition has a strong influence on the magnitude of the maximum Nusselt number. The numerical examination of radiation convection interaction presented by Mezrhab and Bchir (1998) shows that the radiation standardizes the temperature in the two parts of the enclosure. Nishimura *et al.* (1998) studied, both experimentally and numerically, the effect of multiple thin partitions and found that the average Nusselt number is inversely proportional to $(1 + N)$, where N is the number of partitions.

The case where there is a partial or a horizontal partition also received some consideration in the literature. For example, Ciofalo and Karayiannis (1991) investigated the effect of using a fixed-width partition that protrudes centrally from the end-walls of an enclosure on the natural convection. The efficacy of such a partitioning was found to depend upon the aspect ratio and to strengthen as the value of that ratio increases. Yucel and Ozdem (2003) concluded from their numerical investigation on the natural convection in partially divided enclosures that increasing the number of partitions and the height of the partitions causes the average Nusselt number to decrease. Khan and Yao (1993), comparing steady natural convection of water and air in a partially divided enclosure, suggest that the average Nusselt number obtained for water is slightly higher than that obtained for air in the same conditions. Convection in a partially divided enclosure with a combined horizontal temperature and concentration gradient was investigated by Wang *et al.* (2000, 2004). Their results indicate that the partition ratio has strong effects on both the mass transfer rate and

the flow pattern. The effect of using a horizontal partition in an enclosure was analyzed by Nag *et al.* (1993) and they found that the higher the value of the position of the partition along the wall the more the attenuation in heat transfer.

It appears from the literature that the vertical partitions generally taken into consideration in the studies related to natural convection in a fully partitioned enclosure are either thin or with a fixed width or centrally located. In addition, in all of the earlier studies, low order methods such as finite difference, finite element and finite volume methods were used to obtain numerical solution of the governing equations, and in general, low order methods need a large number of grid points to ensure a reliable accuracy.

In this study, steady state laminar natural convection heat transfer in a two-dimensional square enclosure divided by a vertical partition of various thicknesses and conductivities and located centrally or off-centrally is examined numerically using a polynomial-based differential quadrature (PDQ) method.

2. Differential quadrature method

The differential quadrature (DQ) method (Shu, 1992, 2000; Belman *et al.*, 1972; Bellman, 1973) is an efficient discretization technique to obtain accurate numerical solutions using considerably small number of grid points. In the DQ method the derivative of a function is approximated by a weighted linear sum of the function values at given grid points. The weighting coefficients do not relate to any special problem and only depend on the grid spacing. Thus, any differential equation can be reduced to a set of algebraic equations using these coefficients. One essential issue pertaining to the method is how to compute the weighting coefficients. In the DQ method, the first and second order derivatives of $f(x)$ at a point x_i are approximated by:

$$f_x(x_i) = \sum_{j=0}^{n} a_{ij} f(x_j) \quad \text{for } i = 0, 1, 2, \ldots, n, \quad f_{xx}(x_i) = \sum_{j=0}^{n} b_{ij} f(x_j) \quad \text{for } i = 0, 1, 2, \ldots, n \tag{1}$$

where n is the number of the grid points, a_{ij} and b_{ij} are the first and second order weighting coefficients, respectively. Bellman *et al.* (1972) proposed two different techniques to determine the weighting coefficients for the first-order derivatives. While the first method is implemented by solving a system of algebraic equations, the second method is realized by a simple algebraic formulation. Since, the grid points can be chosen arbitrarily, the first method is more popular. Its matrix becomes ill-conditioned when the number of grid points is large. Therefore, it is very difficult to obtain weighting coefficients with this method. To overcome this difficulty, Shu and Richards (1992) proposed a PDQ method for the calculation of the weighting coefficients.

2.1 Polynomial-based differential quadrature method

In the PDQ method, it is supposed that the function $f(x)$ is approximated by an nth degree polynomial in the form:

$$f(x) = \sum_{k=0}^{n} c_k x^k \tag{2}$$

Shu and Richards (1992) derived the following explicit formulations to calculate the weighting coefficients:

$$a_{ij} = \frac{M^{(1)}(x_i)}{(x_i - x_j)M^{(1)}(x_j)}, \quad \text{when } j \neq i, \; a_{ii} = -\sum_{k=1,k\neq i}^{n} a_{ik} \tag{3}$$

$$b_{ij} = 2a_{ij}\left(a_{ii} - \frac{1}{(x_i - x_j)}\right), \quad \text{when } j \neq i, \quad b_{ii} = -\sum_{k=1,k\neq i}^{n} b_{ik} \tag{4}$$

where:

$$M^{(1)}(x_i) = \prod_{k=1,k\neq i}^{n} (x_i - x_k) \tag{5}$$

When the coordinates of grid points are known, the weighting coefficients for the discretization of derivatives can be easily calculated from equations (3)-(5).

3. Analysis

A square enclosure that has a vertical partition of a finite thickness with a variable conductivity is considered in the present study (Figure 1). The temperatures of the vertical walls are kept at T_H and T_C. The horizontal walls are assumed to be adiabatic and both sides of the partition are supposed to obey the conjugate heat transfer boundary condition.

In order to normalize governing equations, the following dimensionless variables are used:

$$x = \frac{x^*}{L}, \quad y = \frac{y^*}{L}, \quad x_p = \frac{x_p^*}{L}, \quad r_w = \frac{w}{L}, \quad r_k = \frac{k_f}{k_p} \tag{6}$$

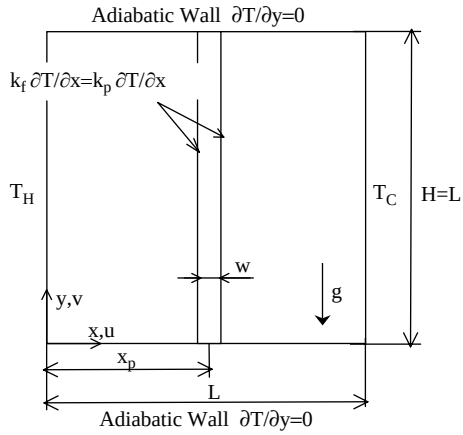

Figure 1.
Geometry and coordinate system

$$u = \frac{u^*}{\alpha/L}, \quad v = \frac{v^*}{\alpha/L}, \quad p = \frac{L^2}{\rho_o \alpha^2}(p^* + \rho_o g y^*), \quad T = \frac{T^* - T_C}{T_H - T_C} \tag{7}$$

where w is the width of the partition, u^* and v^* are the dimensional velocity components, p^* is the dimensional pressure, T^* is the dimensional temperature, ρ is the fluid density and α is the thermal diffusivity of the fluid. The thermal conductivities of the fluid and of the partition are k_f and k_b, respectively. The thermal conductivity ratio and the dimensionless thickness of the partition are r_k and r_w, respectively. As shown in detail by Gill (1966), the scaling equations (6) and (7) is based on the balance between the convective and conductive terms in energy equation, and on the balance between the buoyancy and diffusion terms in momentum equation.

The fluid is assumed to be incompressible with constant properties in the present study. The buoyancy effects are incorporated to the formulation by invoking the Boussinesq approximation. The viscous dissipation terms and the thermal radiation are neglected. With the foregoing assumptions, the dimensionless governing equations for the two dimensional steady state case can be stated as follows in the vorticity-stream function formulation:

$$\frac{\partial^2 \psi}{\partial x^2} + \frac{\partial^2 \psi}{\partial y^2} = -\omega \tag{8}$$

$$u\frac{\partial \omega}{\partial x} + v\frac{\partial \omega}{\partial y} = Pr\left(\frac{\partial^2 \omega}{\partial x^2} + \frac{\partial^2 \omega}{\partial y^2}\right) + RaPr\frac{\partial T}{\partial x} \tag{9}$$

$$\begin{aligned} u\frac{\partial T}{\partial x} + v\frac{\partial T}{\partial y} &= \frac{\partial^2 T}{\partial x^2} + \frac{\partial^2 T}{\partial y^2} \quad \text{(for the fluid)} \\ \frac{\partial^2 T}{\partial x^2} + \frac{\partial^2 T}{\partial y^2} &= 0 \quad \text{(for the partition)} \end{aligned} \tag{10}$$

Here the Prandtl and Rayleigh numbers are defined as:

$$Pr = \frac{\upsilon}{\alpha}, \quad Ra = \frac{g\beta L^3 \Delta T^*}{\upsilon \alpha} \tag{11}$$

where g is the gravitational acceleration, β is the coefficient of thermal expansion and υ is the kinematic viscosity of the fluid. ΔT^* is the temperature difference between the vertical walls of the enclosure.

The dimensionless stream function and vorticity in equations (8) and (9) are defined as follows:

$$u = \frac{\partial \psi}{\partial y}, \quad v = -\frac{\partial \psi}{\partial x}, \quad \omega = \frac{\partial v}{\partial x} - \frac{\partial u}{\partial y} \tag{12}$$

The appropriate boundary conditions for the governing equations are:

$$\psi(x,0) = 0, \quad \left.\frac{\partial T}{\partial y}\right|_{x,0} = 0, \quad \psi(x,1) = 0, \quad \left.\frac{\partial T}{\partial y}\right|_{x,1} = 0 \tag{13}$$

$$\psi(0,y)=0, \quad T(0,y)=1, \quad \psi(1,y)=0, \quad T(1,y)=0 \tag{14}$$

$$\psi(x_p-0.5r_w,y)=0, \quad \left.\frac{\partial T_p}{\partial x}\right|_{x_p-0.5r_w,y}=r_k\left.\frac{\partial T}{\partial x}\right|_{x_p-0.5r_w,y} \tag{15}$$

$$\psi(x_p+0.5r_w,y)=0, \quad \left.\frac{\partial T_p}{\partial x}\right|_{x_p+0.5r_w,y}=r_k\left.\frac{\partial T}{\partial x}\right|_{x_p+0.5r_w,y} \tag{16}$$

There is no physical boundary condition for the value of the vorticity on a solid boundary. However, an expression can be derived from the stream function equation as $\omega_{\text{wall}}=-\partial^2\psi/\partial\eta^2$, where η is the outward direction normal to the surface.

In equations (8)-(16), four governing parameters appear: the Rayleigh number Ra, the partition location x_p, the partition thickness r_w and the thermal conductivity ratio r_k.

The heat transfer results are expressed in the form of the local Nusselt number defined as:

$$Nu=-\left.\frac{\partial T}{\partial\eta}\right|_{\eta=0} \tag{17}$$

4. Numerical procedure

As equations (8)-(10) are coupled and nonlinear partial differential equations, they are solved numerically. The PDQ method with the non-uniform Chebyshev-Gauss-Lobatto grid point distribution given below is used to transform the governing equations into a set of algebraic equations:

$$x_i=\frac{1}{2}\left[1-\cos\left(\frac{i}{n_x}\,\pi\right)\right], \quad i=0,1,2,\ldots,n_x, \quad y_j=\frac{1}{2}\left[1-\cos\left(\frac{j}{n_y}\,\pi\right)\right], \quad j=0,1,2,\ldots,n_y \tag{18}$$

The points in this grid system are more closely spaced in regions near the walls where the higher velocity and temperature gradients are expected to develop. After the numerical discretization, the resulting algebraic equations are solved by the successive over-relaxation iteration method. In order to avoid divergence in the solution of the vorticity equations, an under-relaxation parameter is employed. The convergence criteria is chosen as $|R|_{\max}\leq 10^{-6}$, where $|R|_{\max}$ is the maximum absolute residual values for the vorticity, stream function and temperature equations.

A grid independence study is conducted using five different grid sizes of 21 × 21, 26 × 26, 31 × 31, 36 × 36, 41 × 41 and it is observed that a further refinement of grid from 36 × 36 does not have a significant effect on the results in terms of the average Nusselt number. The results in the case of $Ra=10^6$, $x_p=0.5$, $r_w=0.1$, $r_k=10^{-2}$ are shown in Table I. Based on this observation; a non-uniform grid of 41 × 41 points is used in this study.

In order to validate the numerical code, the predictions for a non-partitioned square enclosure are compared with the benchmark results of de Vahl Davis (1983) through a

standard finite-difference method. The results presented in Table II show that there is an excellent agreement between the results of the present PDQ method for grid 41 × 41 and the benchmark results of Vahl Davis [1,2], which are based on low order methods for grids up to 81 × 81.

5. Results and discussion

Computations are carried out for air as working fluid with a Prandtl number of 0.71. The effect of Rayleigh number is investigated in the range between 10^4 and 10^6. The effect of the thermal conductivity ratio is studied by considering the values between 10^0 and 10^{-3}. Three different values (i.e. 0.1, 0.2, 0.3) are taken for the thickness of the partition. The five different values selected for the location of the partition are 0.1, 0.2, 0.3, 0.4, 0.5.

The results presented below include representative streamline and isotherm patterns; the temperature along the partition; and the local and average Nusselt numbers along the hot surface.

5.1 Streamline and isotherm patterns

Figures 2-4 show the streamlines and isotherms for the case where the partition is in the middle of the enclosure for various values of the thermal conductivity ratio. As it may be observed that, the flow pattern in both regions of the enclosure is characterized by a single cell. The hot fluid particles rise along the hot walls because of buoyancy forces until they reach near the top wall where they turn towards the cold walls while they are cooled. Then they turn downward near those walls. Finally, the restriction imposed by the bottom wall forces the fluid particles to turn towards the hot walls. The flow paths are completed as the colder fluid particles are entrained to the ascending flows. For $Ra = 10^4$, circulation is so weak that the viscous forces are dominant over the buoyancy forces. This causes the conduction to be dominant heat transfer mechanism inside the enclosure. The development of boundary layer flow regime with

Grid pattern	Hot wall Nu_a	Partition wall Nu_a	Cold wall Nu_a
21 × 21	3.85	3.90	3.85
26 × 26	3.88	3.90	3.88
31 × 31	3.90	3.92	3.90
36 × 36	3.92	3.92	3.92
41 × 41	3.92	3.92	3.92

Table I. Effect of the grid size for $Ra = 10^6$, $x_p = 0.5$, $r_w = 0.1$ and $r_k = 10^{-2}$

	$Ra = 10^4$		$Ra = 10^5$		$Ra = 10^6$	
	Vahl Davis	Present	Vahl Davis	Present	Vahl Davis	Present
ψ_{max}	–	5.07	9.61	9.57	16.75	16.76
Nu_a	2.24	2.24	4.52	4.52	8.80	8.82
Nu_{max}	3.53	3.53	7.72	7.71	17.93	17.53
Nu_{min}	0.59	0.59	0.73	0.73	0.99	0.98

Table II. Validation of the numerical code

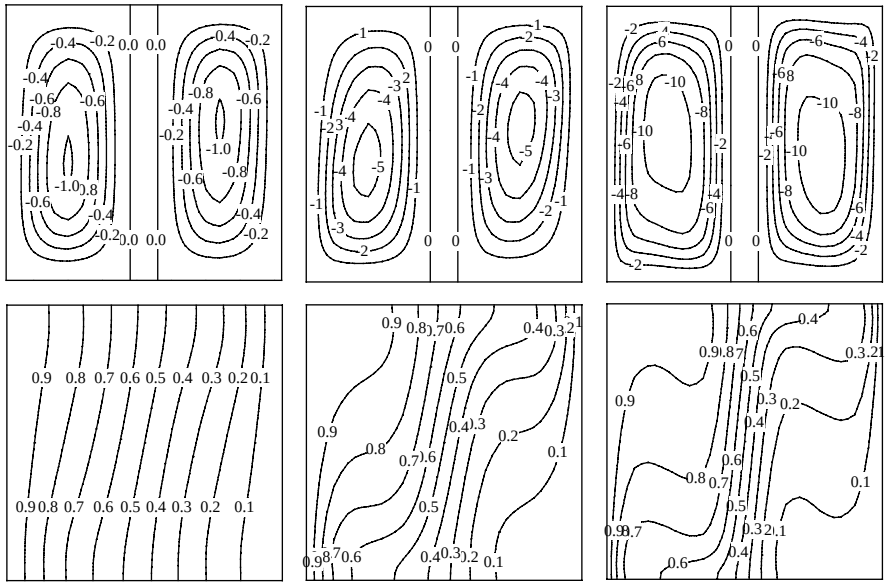

Figure 2.
The streamlines and isotherms for $x_p = 0.5$, $r_w = 0.1$, $r_k = 1$

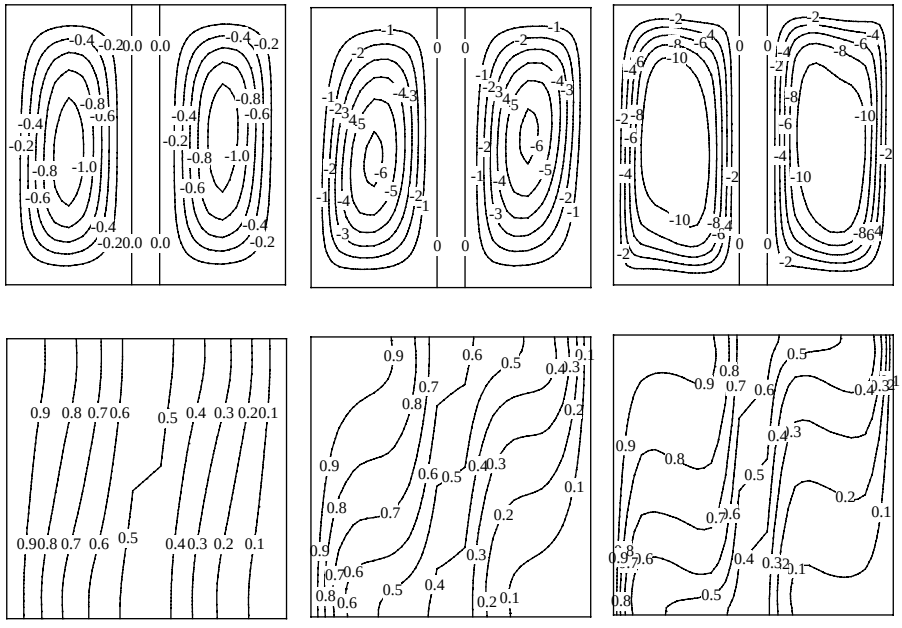

Figure 3.
The streamlines and isotherms for $x_p = 0.5$, $r_w = 0.1$, $r_k = 0.1$

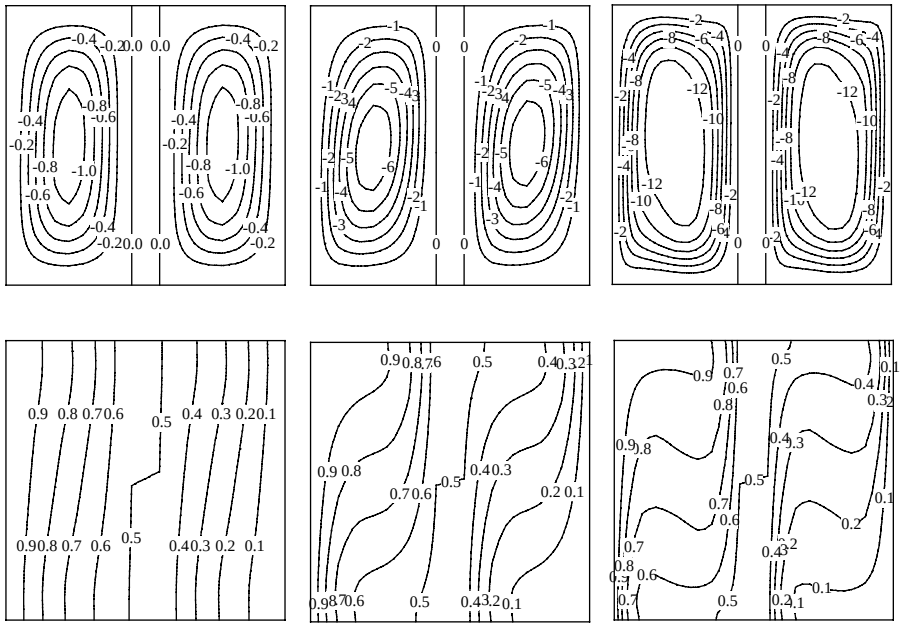

Figure 4.
The streamlines and isotherms for $x_p = 0.5$, $r_w = 0.1$, $r_k = 0.01$

an increasing Rayleigh number is clearly illustrated by the increasing steepness of the temperature profile near the vertical walls, as well as the formation of a plateau in the core region of the two fluid layers. As the thermal conductivity ratio is decreased, an increase in the circulation strength of both regions of the enclosure is seen. However, this effect of the thermal conductivity ratio on the flow diminishes as the thermal conductivity ratio gets lower values.

The effect of the partition thickness on the streamlines and isotherms is shown in Figures 4 and 5. As the partition thickness increases, the circulation strength in both regions decreases to a certain extent due to the narrowing of the flow regions, particularly in the case of low Rayleigh numbers. Distortion in the isotherms also declines to a certain extent in connection with the weakening of the circulation strength.

The streamlines and isotherms for the different partition locations are shown in Figures 4, 5 and 7. Placing the partition the same distance from the cold wall as from the hot wall yielded nearly the same results, only those for $x_p \leq 0.5$ are presented. As it can be seen, when the partition is drawn near the hot wall, the circulation strength weakens in the smaller region. This case indicates that the conductive effect increases in this smaller region. The larger region, however, experiences an increased circulating strength. This phenomenon indicates that the convection effect increases in this region (Figures 6 and 7).

5.2 Partition temperature

The vertical temperature distribution in the middle of the partition is shown in Figure 8(a) for various values of the Rayleigh number. The lower part of the partition is washed by the fluid cooled by the cold wall, while the upper part receives the heated

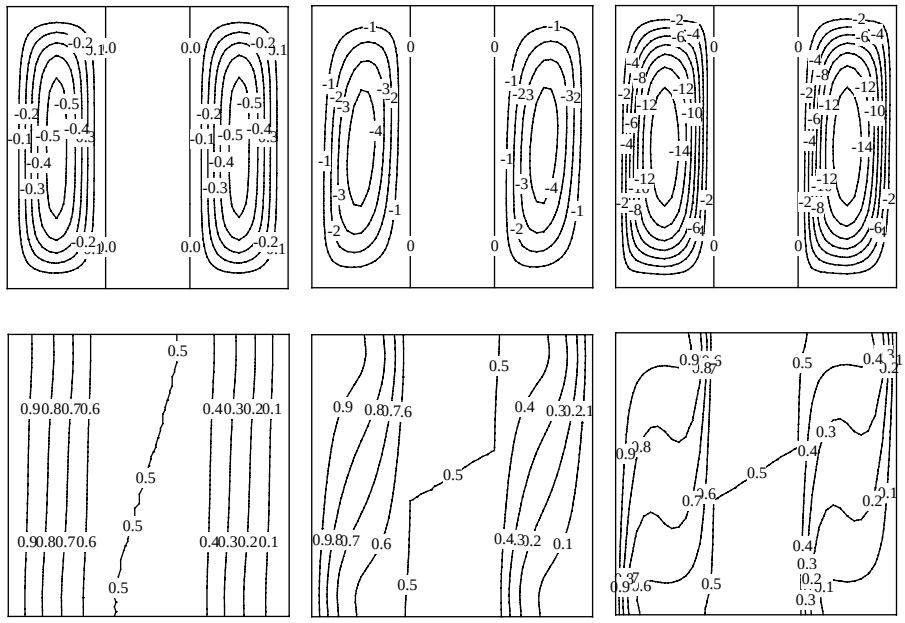

Figure 5.
The streamlines and isotherms for $x_p = 0.5$, $r_w = 0.3$, $r_k = 0.01$

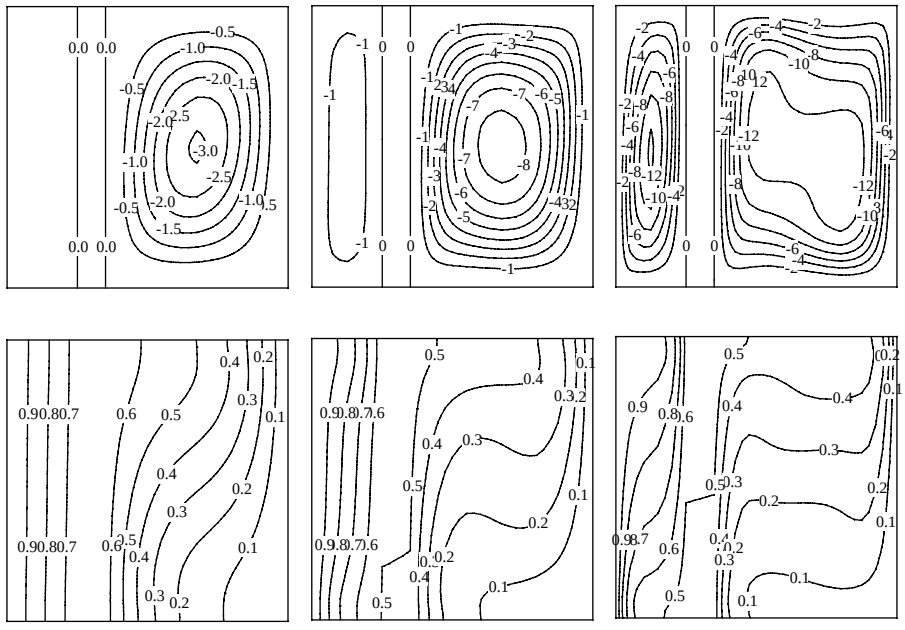

Figure 6.
The streamlines and isotherms for $x_p = 0.1$, $r_w = 0.1$, $r_k = 0.01$

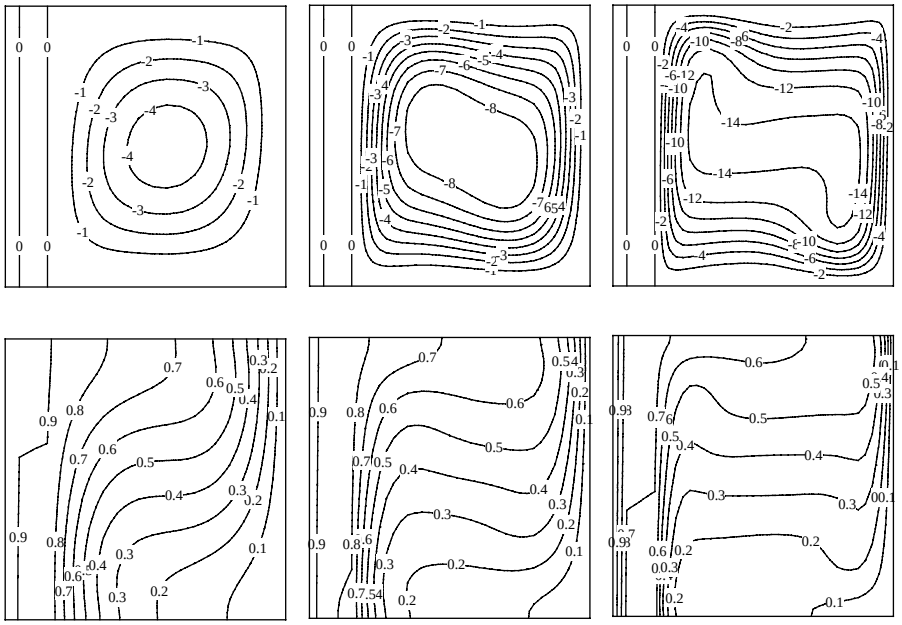

Figure 7.
The streamlines and isotherms for $x_p = 0.3$, $r_w = 0.1$, $r_k = 0.01$

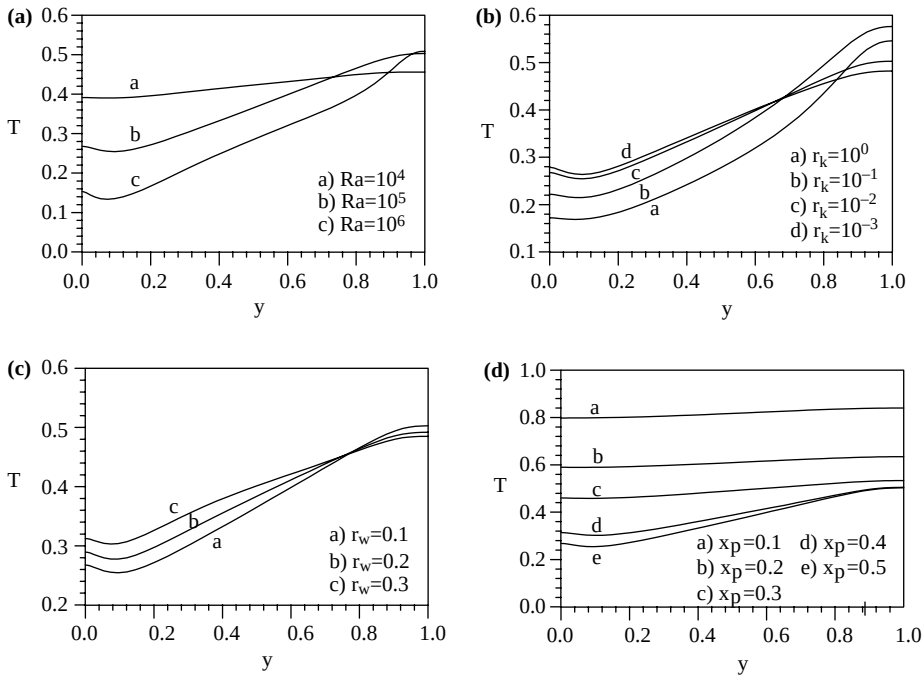

Figure 8.
The variation of the partition temperature for (a) $x_p = 0.5$, $r_w = 0.1$, $r_k = 0.01$; (b) $x_p = 0.5$, $r_w = 0.1$, $Ra = 100{,}000$; (c) $x_p = 0.5$, $r_k = 0.01$, $Ra = 100{,}000$; (d) $r_w = 0.1$, $r_k = 0.01$, $Ra = 100{,}000$

fluid from the hot wall. Therefore, the partition tends to be hotter at the top than at the bottom. The non-uniformity in the temperature distribution along the partition is the smallest at $Ra = 10^4$ and the largest at $Ra = 10^6$. This is expected, since, at $Ra = 10^4$, the natural convection motion is weak and, therefore, the departure of the partition temperature from conduction value of 0.5 is small. As the Rayleigh number increases, the convection motion becomes stronger with the boundary layers developing on the vertical walls. As a result, the departure of the partition temperature from the conduction value increases.

The dependence of the partition temperature on the thermal conductivity ratio is shown in Figure 8(b). For the high values of the thermal conductivity ratio, the conductivity of the partition is relatively small and consequently, a non-uniform temperature profile is attained along it. As the thermal conductivity ratio is decreased, heat flows from the top to the bottom of the partition more easily due to the weaker thermal resistance of the partition, and an almost isothermal temperature profile is attained along the partition.

The variation of the temperature along the partition is shown in Figure 8(c) for various partition thicknesses. As the partition thickness increases, it can be observed that its temperature decreases to a certain extent because of the weakening convective circulation in both regions of the enclosure.

As it can be seen in Figure 8(d), with an increase in the distance between the hot wall and partition, an expected decrease of the partition temperature is seen.

5.3 Local Nusselt number

The variation of the local Nusselt number along the hot wall is shown in Figure 9(a) for various values of the Rayleigh number. It may be observed that the local Nusselt number is strongly dependent on the Rayleigh number and the heat transfer rate increases considerably as the Rayleigh number increases. The local Nusselt number attains its maximum value close to the leading edge of the hot wall. This is expected since the leading edge of the hot wall is washed by the fluid cooled by the partition. The temperature of the fluid moving up the hot wall increases and, therefore, the local Nusselt number decreases as the vertical coordinate increases.

The effect of the thermal conductivity ratio on the local Nusselt number along the hot wall is seen in Figure 9(b). The partition acts like an isolator for the high thermal conductivity ratios. As mentioned previously, with the decrease of the thermal conductive ratio, the thermal resistance of the partition weakens and the thermal interaction between the regions increases. Thus, the local Nusselt number begins to increase. When the thermal conductivity ratio is sufficiently decreased, it reaches degrees that reveal an increase of the temperature in the lower part of the partition. Thus, the horizontal temperature gradient decreases in the lower part of the left region, and the local Nusselt number takes lower values in the lower part of the hot wall.

When analyzing Figure 9(c), in which the variation of the local Nusselt number along the hot wall is shown for various partition thicknesses, it can be seen that the partition thickness has little effect on the heat transfer rate.

Figure 9(d) shows the variation of the local Nusselt number along the hot wall for various values of the partition location. As the distance between the partition and the hot wall decreases, the local Nusselt number gets lower values and becomes uniform

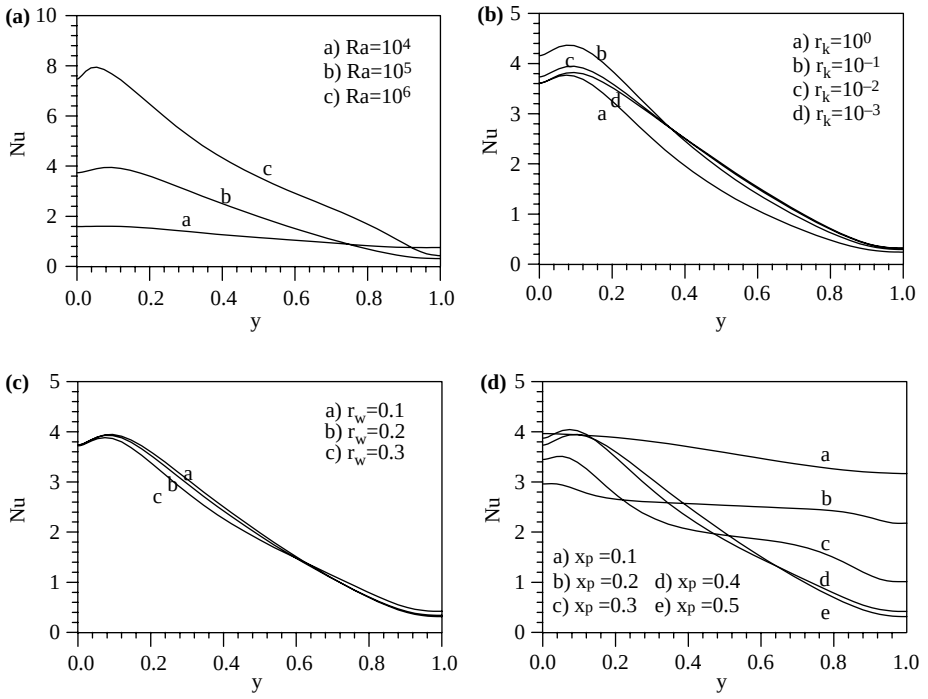

Figure 9.
The variation of the local Nusselt number for (a) $x_p = 0.5$, $r_w = 0.1$, $r_k = 0.01$; (b) $x_p = 0.5$, $r_w = 0.1$, $Ra = 100{,}000$; (c) $x_p = 0.5$, $r_k = 0.01$, $Ra = 100{,}000$; (d) $r_w = 0.1$, $r_k = 0.01$, $Ra = 100{,}000$

since the strength of the convective circulation decreases in the smaller region of the enclosure.

5.4 Average Nusselt number

The primary quantity of practical interest is the average Nusselt number. Since, the average Nusselt number at a surface represents the total heat transferred at the surface, the magnitudes of the average Nusselt number at the hot wall, at the partition and at the cold wall is identical. Therefore, in the following discussion, the results for the average Nusselt number are presented only for the hot wall.

Figure 10 shows the variation of the average Nusselt number with the Rayleigh number for various values of the partition location. In comparison to the non-partitioned case, the results indicate that the vertical partition reduces the convective heat transfer up to 57 percent in the range of Rayleigh number taken into consideration.

The effect of the partition location on the average Nusselt number is shown in Figure 11 for various values of the Rayleigh number. As the distance between the partition and the hot wall increases, the average Nusselt number begins to decrease, and gradually approaches a nearly constant value towards the centre of the enclosure. This trend is similar to that reported numerically in the past by Tong and Gerner (1986). As it may be observed from Figure 11, with a decrease in the Rayleigh number, the effect of the partition location becomes less significant. This is because, at the low

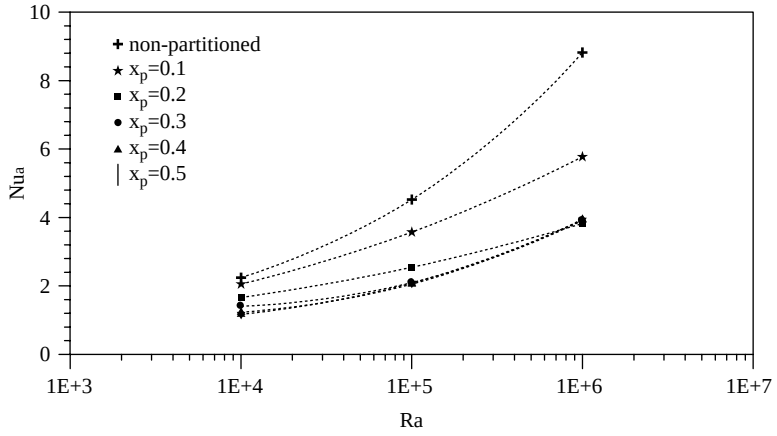

Figure 10.
The variation of the average Nusselt number with the Rayleigh number for $r_w = 0.1$ and $r_k = 0.01$

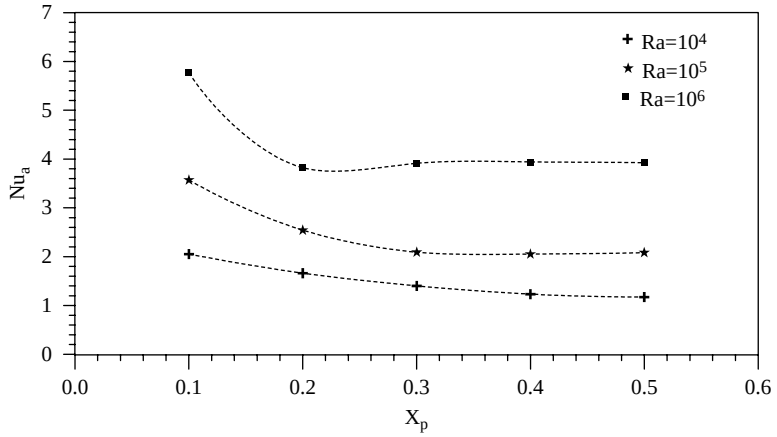

Figure 11.
The variation of the average Nusselt number with the partition location for $r_w = 0.1$ and $r_k = 0.01$

Rayleigh numbers, the heat transfer mechanism is conduction-dominated and, therefore, the effect of the partition location is not so important as that at the high Rayleigh numbers. Furthermore, at the high Rayleigh numbers, the effect of the partition location becomes less significant as the partition gets closer to the centre of the enclosure. For example, the average Nusselt numbers with the partition location from $x_p = 0.2$ to 0.5 are almost of the same values for $Ra = 10^6$. This is because the convection strength does not change significantly for those values of the partition location.

Figure 12 shows the variation of the average Nusselt number with the thermal conductivity ratio for different values of the Rayleigh number. As the thermal conductivity ratio decreases, the average Nusselt number shows a significant increase and a peak point is detected. Beyond the peak point, the average Nusselt number begins to decrease and eventually approaches a constant value. For the high values of the thermal conductivity ratio, the energy within the system is transported from the right to the left almost exclusively by conduction. As the thermal conductivity ratio decreases, convection in each fluid layer is favored and consequently the average Nusselt number

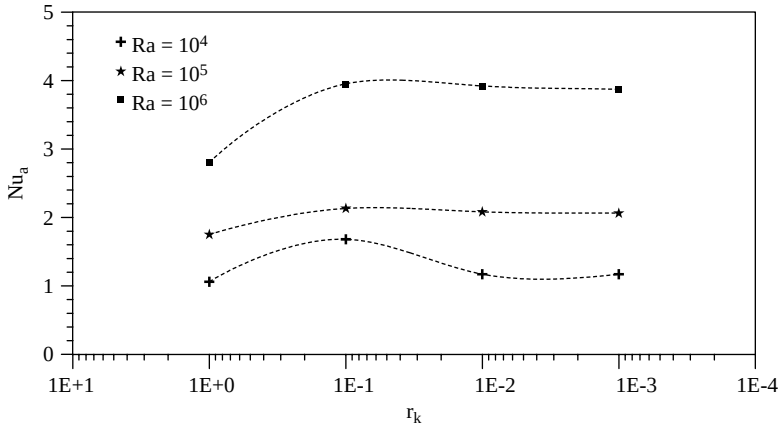

Figure 12.
The variation of the average Nusselt number with the thermal conductivity ratio for $x_p = 0.5$ and $r_w = 0.1$

begins to increase. In the event that the thermal conductivity ratio is decreased by more than a certain extent, there is a decrease of the horizontal temperature gradient in the lower part of the left region due to an increase of the temperature in the lower part of the partition. Thus, the increasing trend appearing in the average Nusselt number depending upon the decreasing thermal resistance of the partition gives its place to the decreasing trend.

It may be observed from Figure 13 that the partition thickness has little effect on the average Nusselt number in the range of the Rayleigh number taken into consideration.

Various correlations for the average Nusselt number are available in the literature for the partitioned enclosures. Duxbury (1979) gives one of them, which is for the isothermal partition, as:

$$Nu_a = 0.143 Ra^{0.25} \left(\frac{H}{L}\right)^{-0.25} \tag{19}$$

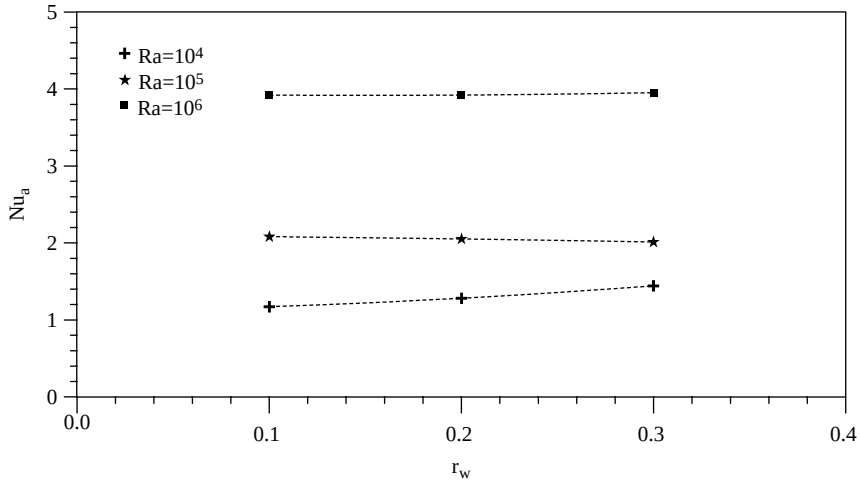

Figure 13.
The variation of the average Nusselt number with the partition thickness for $x_p = 0.5$ and $r_k = 0.01$

In fact, the partition is not isothermal, and its temperature changes in the vertical direction due to the thermal stratification of the fluid within both cells divided by the partition. Nishimura *et al.* (1998) suggests the following correlation based on non-isothermal model:

$$Nu_a = 0.149Ra^{0.25}\left(\frac{H}{L}\right)^{-0.25} \tag{20}$$

The comparison of the results for the predictions obtained in this study using the PDQ method with the results for the correlations given above is presented in Table III. The difference between the results of the present study and the results of the correlations of Duxbury (1979) and Nishimura *et al.* (1998) is because of that these correlations are for a zero width partition and that the correlation of Duxbury (1979) is for an isothermal partition.

Based on numerical calculations carried out, the following correlation is developed for calculating the average Nusselt number covering the governing parameters taken into consideration in this study:

$$Nu_a = (0.115 + 0.006r_k - 0.023r_k^2)Ra^{0.256}x_p^{-0.044} \tag{21}$$

Since, it is found that the contribution of the thickness of the partition is negligible, the thickness of the partition is not correlated. As it can be seen from equation (21) that the corresponding coefficients of developed correlation are similar to the previously developed correlations. This is because of the fact that the correlations are for similar configuration.

6. Conclusion

In this study, natural convection in a partitioned enclosure is investigated numerically. The PDQ method is used for the discretization of the derivatives in the governing equations and in the boundary conditions. The results show that the presence of a vertical partition in the enclosure has a considerable effect on the convective circulation, and hence, the heat transfer characteristics across the enclosure. The average Nusselt number decreases toward a constant value as the distance between the hot wall and the partition increases. As the thermal conductivity ratio decreases, the average Nusselt number increases and a peak point is detected. If the thermal conductivity ratio decreases to a further extent, the average Nusselt number begins to decrease. Furthermore, the average Nusselt number exhibits little dependence on the thickness of the partition in the range taken into consideration in this study for the thickness of the partition. The present method is validated by comparing its numerical results for the average Nusselt number with the results of the correlations available in

Table III.
Comparison of the average Nusselt number predictions with the correlation results given in the literature

	$Ra = 10^4$	$Ra = 10^5$	$Ra = 10^6$
Present study	1.17	2.08	3.92
Isothermal partition model	1.43	2.53	4.51
Nishimura *et al.*	1.49	2.64	4.70

the literature. In addition, a correlation covering the governing parameters in this study is developed for the average Nusselt number.

Note

1. A comprehensive overview of the published results is offered by Ostrach (1988) and Yang (1987).

References

Acharya, S. and Tsang, C.H. (1985), "Natural convection in a fully partitioned inclined enclosure", *Numerical Heat Transfer*, Vol. 8, pp. 407-28.

Belman, R.E., Kashef, B.G. and Casti, J. (1972), "Differential quadrature: a technique for the rapid solution of nonlinear partial differential equations", *Journal of Computational Physics*, Vol. 10, pp. 40-52.

Bellman, R.E. (1973), *Methods of Non-linear Analysis*, Academic Press, New York, NY.

Ciofalo, M. and Karayiannis, T.G. (1991), "Natural convection heat transfer in a partially-or completely-partioned vertical rectangular enclosure", *International Journal of Heat and Mass transfer*, Vol. 34, pp. 167-79.

de Vahl Davis, G. (1983), "Natural convection in a square cavity", *International Journal of Numerical Methods Fluids*, Vol. 3, pp. 249-64.

Duxbury, D. (1979), "An interferometric study of natural convection in enclosed plane air layers with complete and partial central vertical divisions", PhD thesis, University of Salford, Salford.

Dzodzo, D.M.C., Dzodzo, M.B. and Pavlovic, M.D. (1999), "Laminar natural convection in a fully partitioned enclosure containing fluid with nonlinear thermophysical properties", *International Journal of Heat and Fluid Flow*, Vol. 20, pp. 614-23.

Gill, A.E. (1966), "The boundary layer regime for convection in a rectangular cavity", *Journal of Fluid Mechanics*, Vol. 26, pp. 515-36.

Ho, C.J. and Yih, Y.L. (1987), "Conjugate natural heat transfer in an air-filled rectangular cavity", *International Communication in Heat and Mass Transfer*, Vol. 14, pp. 91-100.

Karayiannis, T.G., Ciofalo, M. and Barbaro, G. (1992), "On natural convection in a single and two zone rectangular enclosure", *International Journal of Heat and Mass Transfer*, Vol. 35 No. 7, pp. 1645-57.

Khan, J.A. and Yao, G-F. (1993), "Comparison of natural convection of water and air in a partitioned rectangular enclosure", *International Journal of Heat and Mass Transfer*, Vol. 36 No. 12, pp. 3107-17.

Mezrhab, A. and Bchir, L. (1998), "Radiation-natural convection interactions in partitioned cavities", *International Journal of Numerical Methods for Heat & Fluid Flow*, Vol. 8 No. 7, pp. 781-99.

Nag, A., Sarkar, A. and Sastri, V.M.K. (1993), "Natural convection in a differentially heated square cavity with a horizontal partition plate on the hot wall", *Computer Methods in Applied Mechanics and Engineering*, Vol. 110 No. 7, pp. 143-56.

Nishimura, T., Shiraishi, M., Nagasawa, F. and Kawamura, Y. (1998), "Natural convection heat transfer in enclosures with multiple vertical partitions", *International Journal of Heat and Mass Transfer*, Vol. 31, pp. 1679-998.

Ostrach, S. (1988), "Natural convection in enclosures", *Journal of Heat Transfer*, Vol. 2, pp. 1175-90.

Shu, C. (1992), "Generalised differential-integral quadrature and application to the simulation of incompressible viscous flows including parallel computation", PhD thesis, University of Glasgow, Glasgow.

Shu, C. (2000), *Differential Quadrature and its Application in Engineering*, Springer, Berlin.

Shu, C. and Richards, B.E. (1992), "Application of generalized differential quadrature to solve two-dimension incompressible Navier Stokes equations", *International Journal for Numerical Methods in Fluids*, Vol. 15, pp. 791-8.

Tong, T.W. and Gerner, F.M. (1986), "Natural convection in partitioned air-filled rectangular enclosures", *International Communication in Heat and Mass Transfer*, Vol. 10, pp. 99-108.

Wang, L.W., Deng, Z.F., Wang, S.L. and Kung, Y.C. (2000), "Thermosolutal convection in a partially divided square", *Experimental Heat Transfer*, Vol. 13 No. 3, pp. 211-22.

Wang, L.W., Kung, Y.C., Wu, C.Y. and Kang, M.F. (2004), "Thermosolutal convection in an inclined rectangular enclosure with a partition", *Journal of Mechanics*, Vol. 20 No. 3, pp. 233-9.

Yang, K.J. (1987), "Natural convection in enclosures", *Handbook of Single-phase Convective Heat Transfer*, 3, Wiley, New York, NY.

Yucel, N. and Ozdem, A.H. (2003), "Natural convection in partially divided square enclosures", *Heat and Mass Transfer*, Vol. 40 Nos 1/2, pp. 167-75.

Corresponding author
Kamil Kahveci can be contacted at: kamilk@trakya.edu.tr